Organic & Biomolecular Chemistry

PAPER

View Article Online
View Journal

Cite this: DOI: 10.1039/c6ob02559e

Glyco-functionalized dinuclear rhenium(I) complexes for cell imaging†

Alessandro Palmioli,‡§[a] Alessandro Aliprandi,§[b] Dedy Septiadi,§[b] Matteo Mauro,*[b] Anna Bernardi,[a] Luisa De Cola[b] and Monica Panigati*[a,c,d]

Received 22nd November 2016,
Accepted 19th January 2017

DOI: 10.1039/c6ob02559e

rsc.li/obc

The design, synthesis and photophysical characterization of four new luminescent glycosylated luminophores based on dinuclear rhenium complexes, namely Glyco-Re, are described. The derivatives have the general formula $[Re_2(\mu\text{-}Cl)_2(CO)_6(\mu\text{-pydz-R})]$ (R-pydz = functionalized 1,2-pyridazine), where a sugar residue (R) is covalently bound to the pyridazine ligand in the β position. Different synthetic pathways have been investigated including the so-called neo-glycorandomization procedure, affording stereoselectively glyco-conjugates containing glucose and maltose in a β anomeric configuration. A multivalent dinuclear rhenium glycodendron bearing three glucose units is also synthesized. All the Glyco-Re conjugates are comprehensively characterized and their photophysical properties and cellular internalization experiments on human cervical adenocarcinoma (HeLa) cells are reported. The results show that such Glyco-Re complexes display interesting bio-imaging properties, *i.e.* high cell permeability, organelle selectivity, low cytotoxicity and fast internalization. These findings make the presented Glyco-Re derivatives efficient phosphorescent probes suitable for cell imaging application.

Introduction

Carbohydrates play a crucial role in different important biological processes such as cell proliferation and differentiation as well as cellular immune response. Therefore monitoring their uptake process and distribution inside cellular compartments is of fundamental importance for the diagnosis of various diseases and for developing new therapeutic agents.[1]

Luminescent organometallic complexes based on second and third row transition metals possess unique spectroscopic and photophysical properties, such as high emission quantum yield, photostability, long-lived excited states and sensitivity to the surrounding environment. Nowadays, all these features have been advantageously employed for bio-imaging purposes and this research topic has been attracting a great deal of attention due to potential scientific fall-outs in biology, biochemical and medical research.[2] Moreover, metal complexes could be endowed with high photoluminescence quantum yields even in air-equilibrated aqueous media and relatively long lifetimes by appropriate molecular design. Furthermore, they may exhibit low toxicity and good cellular internalization features.[3]

In this respect, synergic combination of biomolecules, such as carbohydrates, with transition-metal complexes to generate luminescent bioconjugates represents a promising strategy to obtain sensitive molecular tools to gain deeper insight into biological key-events such as cellular internalization processes, metabolism and biodistribution.

Due to their high water solubility, carbohydrates can be favorably used to effectively solubilize apolar structures in polar media. Furthermore, it is now well established that carbohydrates are involved in a variety of molecular recognition phenomena of physiological and pathological relevance in living organisms that could be imaged using glycosylated luminescent probes.[1b]

Various luminescent transition-metal glycoconjugate complexes based on zinc,[4] ruthenium(II),[5] iridium(III)[6] and platinum(II)[7] have been recently reported and amongst them phosphorescent rhenium(I) tricarbonyl polypyridine complexes are the most extensively studied systems.

Although the use of rhenium(I) glyco-conjugates as biosensors in carbohydrate-related events goes back to 2006,[8] quite surprisingly their application as luminescent probes for

[a]Department of Chemistry, Università degli Studi di Milano, Via Golgi 19, 20133 Milano, Italy. E-mail: monica.panigati@unimi.it; Fax: +39 0250314405; Tel: +30 0250314352
[b]ISIS & icFRC, Université de Strasbourg & CNRS, 8 rue Gaspard Monge, 67000 Strasbourg, France. E-mail: mauro@unistra.fr
[c]Milan Unit of INSTM, Via Golgi 19, 20133 Milano, Italy
[d]Istituto per lo Studio delle Macromolecole, Consiglio Nazionale delle Ricerche (ISMAC-CNR), Via E. Bassini, 15, 20133 Milano, Italy
†Electronic supplementary information (ESI) available. See DOI: 10.1039/c6ob02559e
‡Present address: Università degli Studi di Milano-Bicocca, Dipartimento di Biotecnologie e Bioscienze, Piazza della Scienza 2, 20126 Milano, Italy.
§These three authors contributed equally to the work.

cell imaging has been little exploited to date. Indeed, only three examples have been reported so far in the literature, to the best of our knowledge.[9] Such examples deal with mononuclear cationic complexes, containing either aromatic bipyridyl (bpy) or dipyridophenazine (dppz) ligands, which show cytotoxic activity with an IC_{50} value in the low micromolar range.

In the last few years our groups have developed a novel family of neutral dinuclear rhenium(I) derivatives (see Chart 1) that exhibit intense emission in the visible region, originating from a triplet-manifold excited state being a metal-to-ligand charge transfer (^{3}MLCT) in nature. These neutral derivatives, which can be obtained with good reaction yields, are characterized by two $Re(CO)_3$ units connected by a substituted diazine ligand and two anionic ancillary ligands.[10] Also, modulation of the photophysical properties was promptly achieved by both substituent effects on the diazinic moiety and ancillary bridging ligands, reaching photoluminescence quantum yield values, (Φ), as high as 0.53, when electron-rich diazine ligands were employed and chlorine was chosen as the bridging ligand (X = Cl).[11]

Owing to their highly interesting photophysical features and photostability, including high Φ and the possibility to stimulated them by two-photon excitation techniques, this family of dinuclear complexes have been used as low-toxicity luminescent tags for Peptido Nucleic Acid (PNA) labelling, and successfully tested in cell imaging experiments,[12] showing negligible cytotoxicity and efficient cell uptake in living cells with different kinetics and localization depending on the nature of the PNA chain and of the diazine substituent. The stiff "Re(μ-Cl)$_2$Re" skeleton, which leads to high photoluminescence quantum yields in solution, allowed imaging at a low concentration (25–100 μM), and prevented the release of the chloride ligands which was often responsible for the toxicity as reported for neutral mononuclear diimine rhenium chloride complexes.[13]

These results prompted us to investigate the possibility to develop new luminescent labels for novel glycosylated probes based on these dinuclear rhenium complexes as simple, chemically robust and easy-to-synthesize platforms that can accommodate different carbohydrates.

Using the synthetic approach of the neo-glycorandomization technique,[14] which allows direct functionalization of unprotected sugars in anomeric positions, a series of luminescent glyco-functionalized neutral dinuclear rhenium complexes are prepared. Hereafter, the effects of substituents bound to the diazine ligand, and the length of the spacer as well as nature and number of the conjugated carbohydrates on the photophysical properties are reported. Finally, the intracellular distribution of the complexes by means of laser scanning confocal fluorescent microscopy is discussed.

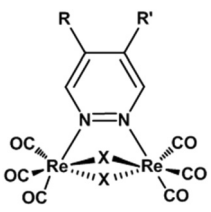

Chart 1 General structure of dinuclear Re(I)-complexes bearing a bridging 1,2-diazine ligand with different alkyl groups (R and R') and two ancillary anionic ligands (X = Cl, Br, I).

Results and discussion

Design and synthesis

Two different dinuclear rhenium complexes (see Chart 2) were selected as starting materials for the synthesis of Glyco-Re derivatives **3–6** aiming to study their solubility, the photophysical behavior and the cellular uptake of these new glyco-conjugates (see Chart 3). Indeed, the length, the degree of branching and the flexibility of the spacer could be important to control the affinity of the resulting conjugate with cell surface receptors. Furthermore, the number and type of connected sugars, as well as the chemical and biological stability of the linker moiety are also crucial factors to consider in the design of the bio-conjugated luminophores.

Complex **1** was already used as a luminescent probe for PNA labelling[12] while the new complex **2**, which contains two alkyl substituents in the β positions of the diazine ring, could provide a hypsochromically shifted emission with a higher quantum yield and longer lifetime compared to the analogous mono-substituted complex **1**.[11] Both complexes were synthesized using the previously reported two-step procedure involving an inverse-type [4 + 2] Diels–Alder cycloaddition reaction between the electron-poor 1,2,4,5-tetrazine and the appropriate functionalized alkynes with N_2 loss.[15] Following our previously reported procedure,[10] the complexes **1** and **2** were prepared by refluxing $[Re(CO)_5Cl]$ with 0.5 equivalents of the corresponding 1,2-diazine in toluene solution.

Complex **3**, consisting of a β-*O*-glucoside derivative of the dinuclear rhenium complex **2**, was synthesized as shown in Scheme 1. Commercial hex-3-ynol **7** was glycosylated with penta-*O*-acetyl-D-glucose **8** and the resulting product **9** was deacetylated under Zemplen conditions, obtaining the β-hex-3-ynyl-1-*O*-β-D-glucopyranoside-alkyne **10**. Alkyne **10** was used for the synthesis of the diazine ligand, following the well-established literature procedure involving an inverse-type [4 + 2] Diels–Alder cycloaddition reaction between the electron-poor 1,2,4,5-tetrazine and the alkyne dienophile, that occur with N_2

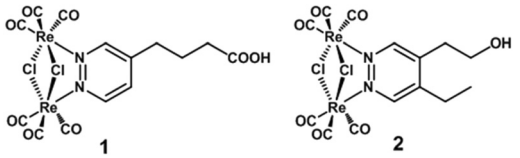

Chart 2 The dinuclear Re complexes **1** and **2** used as luminescent labels.

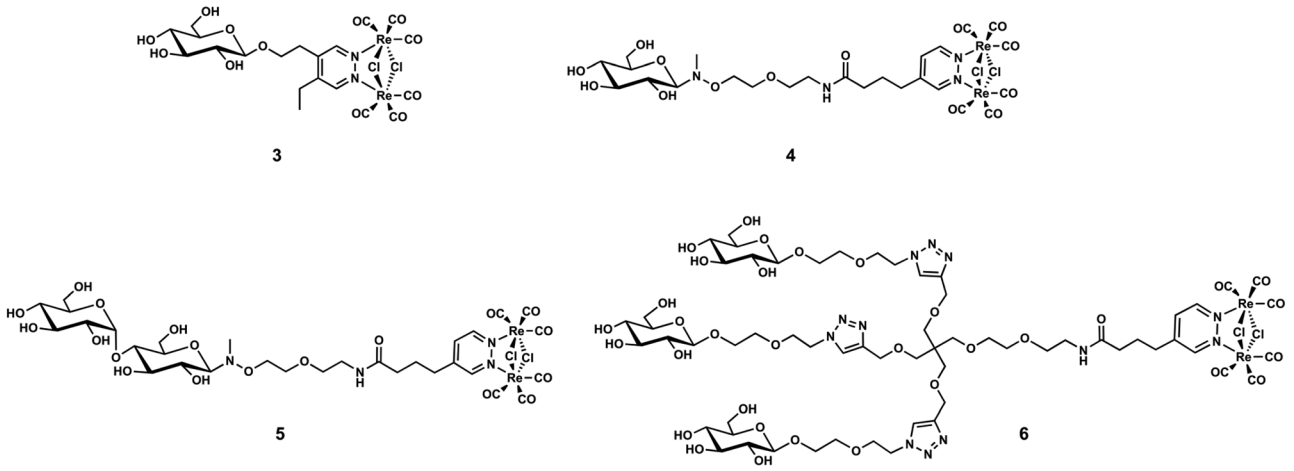

Chart 3 Structure of neutral dinuclear Re-glycoconjugates **3–6** synthesized in this study.

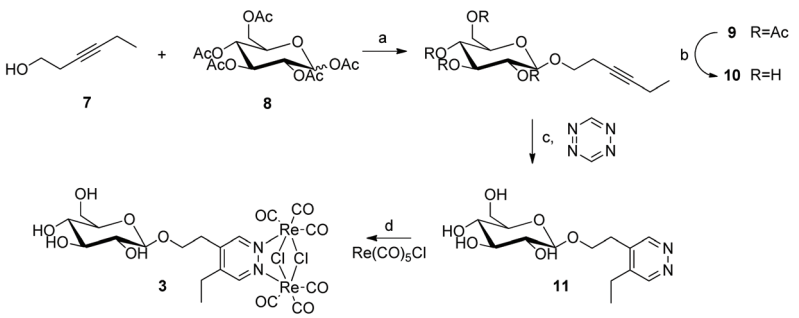

Scheme 1 Schematic synthetic pathway employed for preparing compound **3**. Reagents and conditions: (a) $BF_3{\cdot}Et_2O$, CH_2Cl_2 dry, 0 °C then room temperature, 4 hours, yield 53%; (b) NaOMe 0.1 M, MeOH dry, room temperature, 1 hour, yield 81%; (c) 1,4-dioxane, 80 °C, 24 hours, yield 35%; (d), toluene, reflux, 3 hours, yield 12%.

loss.[15] Finally, the functionalized diazine ligand (**11**) was treated with two equivalents of the organometallic precursor $Re(CO)_5Cl$ obtaining the final β-*O*-D-glucoside-Re complex **3**. Both **3** and the corresponding diazine ligand **11** were isolated and purified by reverse phase chromatography. Complex **3** was isolated as a yellow solid which was found to be soluble at the mM level in organic polar solvents, such as MeOH and DMSO, and in a 1 : 1 $MeOH : H_2O$ mixture. Although all synthetic intermediates and final compounds have been successfully isolated and fully characterized, this synthetic strategy has a poor overall yield, principally because of the last two steps, which have reaction yields of 35% and 12%, respectively.

For this reason the synthetic procedure shown in Scheme 1 was not suitable for the synthesis of a large set of conjugates containing different natural monosaccharides and oligosaccharides. Therefore a bifunctional linker (**16**, see Scheme 2), that bears a primary amino group and an *N*-methylamino-oxy group was developed. It could act as a robust and easily accessible platform, able to accommodate both the photoluminescent tag and the different carbohydrate moieties in a fast, convergent and parallel manner. This linker allowed exploiting the chemoselective glycosylation approach based on the one-step reaction of *N*-methylamino-oxy groups with an unprotected non-activated reducing sugar, affording a neo-glycoconjugate under mild conditions.[16] In addition, the formed neo-glycosidic linkage was quite stable under physiological conditions and toward enzymatic hydrolysis. Overcoming protection/activation/deprotection steps of traditional glycosylation reactions, this method was used for the preparation of the glycoconjugates **4** and **5** as reported in Scheme 2.

The 2-(2-azidoethoxy) ethanol (**13**), obtained from commercial 2-(2-chloroethoxy) ethanol (**12**) and NaN_3 (Scheme 2), was first tosylated (**14**) and then treated with *N*-Boc-*N*-methylhydroxylamine and DBU to afford *N*-Boc-*N*-methyl-2-(2-azidoethoxy)ethoxy hydroxylamine (**15**). Then the azido group was reduced under Staudinger conditions (PPh_3 and water) and the amine **16** was coupled with a dinuclear Re(I) complex **1** affording the intermediate **17a** with a satisfactory overall yield. The *N*-Boc protecting group was removed in the presence of CF_3COOH in CH_2Cl_2 and the resulting *N*-methyl hydroxylamine **17b** was isolated as the trifluoroacetate salt in quantitative yield. Finally, chemoselective glycosylation of **17b** to afford **4** or **5** was performed in the presence of 3 eq. of unprotected reducing sugar (D-glucose or D-maltose, respectively) and

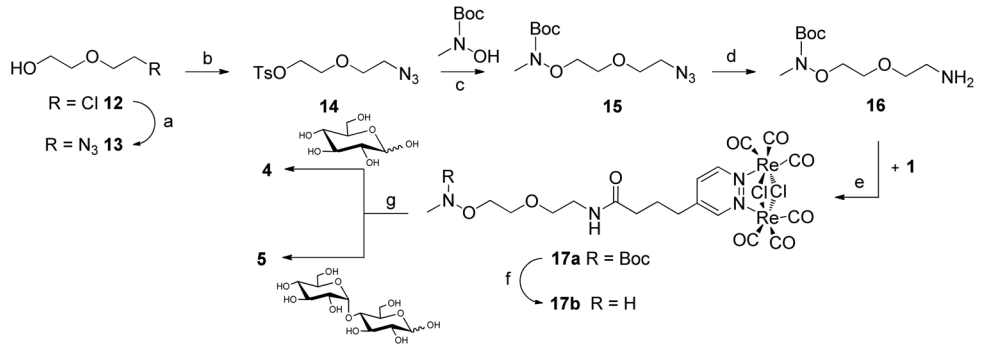

Scheme 2 Schematic synthetic pathways employed for the neoglyco-conjugates **4** and **5**. Reagents and conditions: (a) NaN_3, NaI, H_2O, 60 °C, 4 days, quantitative yield; (b) TsCl, Et_3N, CH_2Cl_2, 0 °C then room temperature, 3 hours, yield 80%; (c) 1,5-diazabiciclo(5.4.0)undec-5-ene (DBU), THF then solvent-free, room temperature, 12 hours, yield 88%; (d) PPh_3, Na_2CO_3, H_2O, CH_2Cl_2, room temperature, 12 hours, yield 85%; (e) HATU, DIPEA, CH_2Cl_2 (5% dry DMA), room temperature, 2 hours, yield 76%; (f) TFA, dry CH_2Cl_2, 1 hour, quantitative yield; (g) D-glucose or maltose, glacial AcOH, dry MeOH, room temperature, 18 hours, yield 62% and 63% for **4** and **5**, respectively.

25 eq. of AcOH in MeOH at room temperature overnight (Scheme 2). The neo-glycoconjugate products were obtained stereoselectively in a β anomeric configuration with satisfactory yields (62% and 63% for **4** and **5**, respectively). Compounds **4** and **5** are both soluble in water in a low mM range concentration.

Finally, for the synthesis of the multivalent glycoconjugate **6** (Scheme 3), the trivalent glucodendron **18** was prepared from commercial pentaerythritol (the full synthetic scheme is reported Scheme S1 of the ESI†) and linked with the dinuclear Re(I) complex **1** using HATU/DIPEA as coupling reagents. The Re(I)-glycodendrimer **6** was purely isolated after reverse-phase C18 chromatography purification. Complex **6** was soluble in water in the mM concentration.

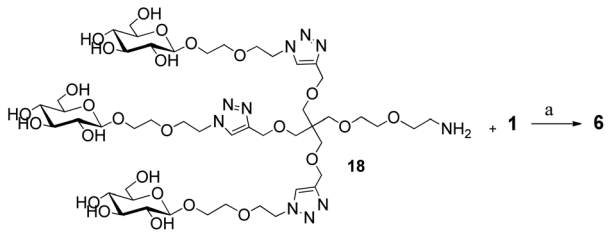

Scheme 3 Synthesis of the multivalent glycoconjugate **6**. Reagents and conditions: (a) 1, HATU, DIPEA, dry DMA, room temperature, 2 hours, yield 68%.

Photophysical characterization

The photophysical properties of the glyco-derivatives **3–5** and of their parent complexes **1** and **2** were studied under dilute condition (concentration of 1.0×10^{-5} M) in both air-equilibrated and deareated 1,4-dioxane solution at room temperature. The multi-functionalized complex **6** was investigated in aqueous solution due to its very low solubility into apolar solvents. The corresponding photophysical data are listed in Table 1.

At longer wavelengths, the electronic absorption spectra of compounds **1–5** in dioxane display a broad absorption band with the maxima in the range 347–359 nm with a moderate intensity ($\varepsilon \approx 0.67$–0.88×10^4 M^{-1} cm^{-1}), whilst complex **6** in distilled H_2O displays an absorption maximum centred at $\lambda_{abs} = 323$ ($\varepsilon \approx 0.55 \times 10^4$ M^{-1} cm^{-1}). Such a transition can be

Table 1 Photophysical properties obtained for compounds **1–6** in both air-equilibrated and deaerated dilute samples at room temperature

Compound		λ_{abs} (ε) (nm, [$\times 10^4$ M^{-1} cm^{-1}])	λ_{em} [nm]	τ [μs]	Φ_{em} (%)	k_r [$\times 10^5$ s^{-1}]	k_{nr} [$\times 10^5$ s^{-1}]
1[a]	Air	359 (0.76)	585	0.378	3		
	Deg	—	585	1.27	8	0.63	7.24
2[a]	Air	348 (0.88)	562	0.458	3		
	Deg	—	562	3.26	20	0.61	2.45
3[a]	Air	347 (0.70)	570	0.451	3		
	Deg	—	570	2.73	19	0.68	2.98
4[a]	Air	352 (0.67)	591	0.419	3		
	Deg	—	588	1.18 (81%), 1.83 (19%)	12	0.66	4.81
5[a]	Air	355 (0.77)	589	0.436	4		
	Deg	—	589	1.36 (97%), 2.88 (3%)	11	0.78	6.36
6[b]	Air	323 (0.55)	594	0.011 (17%), 0.144 (74%), 0.504 (9%)	<1		
	Deg	—	594	0.365 (24%), 0.138 (38%), 0.014 (38%)	<1	0.66	66.0

[a] In 1,4-dioxane. [b] In distilled water.

assigned to the spin allowed dπ(Re) → π*(diazine ring) ^{1}MLCT band, typical of this class of complexes.[10,11] Also, the CT character of such transitions was supported by the modulation on the absorption energy by both substituent effects on the diazine ligand and the solvent polarity. Accordingly, complexes **2** and **3**, featuring a diazine containing two alkyl substituents in the β positions, displayed a blue-shifted absorption band with respect to the mono substituted complexes **1**, **4** and **5**. Indeed, the second electro-donating alkyl chain on the diazine ligand increases the energy level of the LUMO, raising in this way the HOMO–LUMO gap and therefore the energy of the ^{1}MLCT excited state.[11] A hypsochromically shifted absorption band was also observed for complex **6** but, in this case, this feature is most likely due to the much higher polarity of the solvent used (water *vs.* dioxane). It is interesting to note that the conjugation of the carbohydrate on the organometallic scaffold does not modify the absorption properties, as previously observed also for the analogues for PNA-conjugates.[12]

Upon excitation in the range 350–380 nm at room temperature, all the samples showed broad and featureless emission in the yellow-orange region of the visible spectrum, which is assigned to the radiative decay of the ^{3}MLCT excited state, as comparison with closely related complexes (see Fig. 1).[11] In addition, the triplet nature of the radiative transition is further supported by the oxygen quenching effect observed starting from degassed to air-equilibrated samples (Table 1). Similar to what was observed in the absorption spectra, complex **1** and its related glyco-conjugates **4–5** display remarkably different emission features compared to derivatives **2–3**. Indeed, a hypsochromically shifted and more intense emission was recorded for complexes **2–3**, which is accompanied by a higher Φ and longer emission lifetime as a consequence of the higher energy of the ^{3}MLCT excited state (see Table 1). However, for all the complexes the values of Φ/τ, which represents the product between the radiative rate constant (k_r) and the efficiency of intersystem crossing (η_{ICS}), were found in the range of 6.1–7.8 × 10^4 s^{-1}, indicating that the differences observed in the luminescence properties are mainly to be attributed to the efficiency of the nonradiative processes, k_{nr}.

Even if the conjugation with sugar is not expected to directly influence the nature of the excited state, it is interesting to note that deareated Φ and an excited-state lifetime for the glyco-substituted complex **3** were slightly lower than those observed for the non-functionalized benchmark complex **2**. The reason can be likely ascribed to the increased conformational freedom due to the presence of the glucose moiety, which may favour nonradiative deactivation pathways as suggested by the moderate increase of the k_{nr} for complex **3** (see Table 1).

In contrast, different findings were observed for complex **4–5** in comparison with the parental complex **1**. The former showed a higher quantum yield and a slightly longer excited-state lifetime with bi-exponential decay kinetics under de-aerated conditions. This feature is most likely attributed to the formation of soft supramolecular aggregates by establishment of sugar–sugar interactions due to the amphiphilic nature of complexes **4** and **5** upon a freeze–pump procedure. Indeed, the simultaneous presence of the apolar head core, constituted by the dinuclear rhenium complex, and the hydrophilic sugar moiety, connected to each other by a flexible hydrophilic chain, is expected to promote self-organization of the molecules in solution, as recently reported by some of us.[17] It is reasonable to think that such a self-assembling process is further driven by intermolecular hydrogen bonds between the hydroxyl groups of the glucose and maltose moieties in an apolar media such as dioxane, affording large vesicular-like structures with an inverse architecture in which the apolar "$Re(CO)_3$" heads are oriented towards a dioxane solvent media. Thus, the formation of such soft aggregates made by amphiphilic molecules might be responsible for the observed photophysical features.

Additionally, the aggregation tendency of compound **4** and **5** was also confirmed by ^{1}H NMR spectroscopy in a d_4-methanol solution at room temperature. In the ^{1}H NMR spectra of a dilute solution of either **4** or **5** (1 mM) no resonance signal of the N–*H* proton of the amide group of the linker was observed, due to the H-D exchange with the solvent. However, upon increasing the concentration of the complex up to 20 mM, a rise of a triplet signal at about 8.00 ppm, attributed to the N–*H* involved in stable intermolecular *H*-bond interactions, was observed (see Fig. 2).

On the other hand, dilute samples of complex **6** in distilled H_2O display a very different behavior with a rather low photoluminescence with λ_{em} centred at 594 nm and a short-lived excited state even after the degassing procedure.

In aqueous media, the amphiphilic compound **6** with a cone-like shape is expected to aggregate into direct micellar structures in which the apolar heads are oriented internally into the supramolecular architecture. Such a configuration, in which long-lived excited states located onto the organometallic head are closely spaced, is expected to enhance triplet–triplet annihilation processes yielding an increase of radiationless decay channels as demonstrated by the much higher k_{nr} constant observed for **6**.

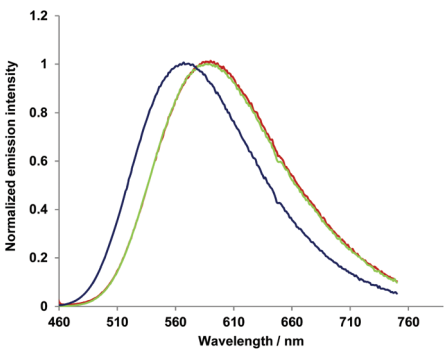

Fig. 1 Normalized emission spectra of complexes **3** (blue trace), **4** (red trace) and **5** (green trace) in deaerated 1,4-dioxane solution at a concentration of 1.0 × 10^{-5} M at room temperature (λ_{ex} 380–400 nm).

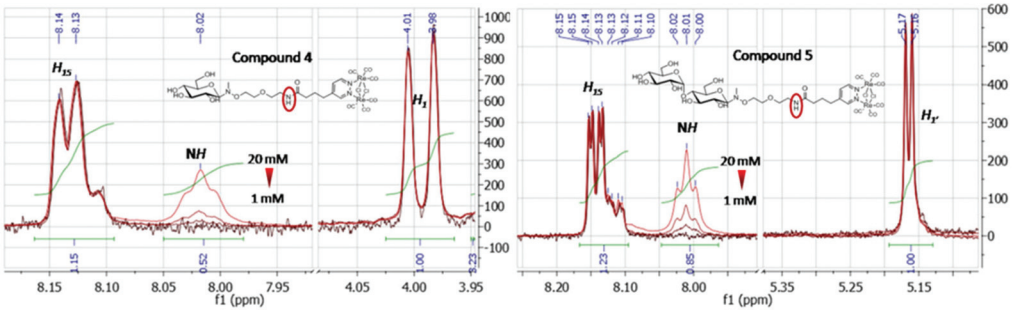

Fig. 2 ^{1}H NMR spectra recorded for compound **4** and **5** in methanol-d_4 at a concentration range from 1 to 20 mM at room temperature. The red symbol shows the variation of the resonance upon increasing the concentration.

Cellular uptake assays

In order to study the internalization and bio-imaging properties of the Glyco-Re(I) complexes as cellular probes, we performed cellular uptake experiments of complexes **3–6** on the human cervical carcinoma (HeLa) cell line. As depicted in Fig. 3 and S3 of the ESI,† compound **3** was internalized by living HeLa cells and accumulated mainly in the cytoplasmic region and the corresponding intracellular emission was centered at 573 nm, as previously observed from photophysical measurements in solution. Complex **4** and **5** display efficient internalization into HeLa cells as well. In order to understand the effect of the initial concentration of the complexes in the staining media on the cellular behaviour at a specific incubation time, we carried out concentration dependent uptake experiments. Expectantly, increasing the concentration of the emitting complex into the staining solution from 25 to 100 μM results in an increase of the number of internalized molecules as can be noticed through increment of emission intensity signals. The results are displayed in Fig. 4 and S4 of the ESI† for compound **4** and **5**, respectively. The corresponding intensity profile recorded for different concentrations of compound **4** in the incubating media is displayed in Fig. S5a of the ESI.†

Overall, we also found that there is no significant difference in terms of intracellular distribution of the complexes since for example migration of the luminescent probe towards the nuclear region was not observed at the highest concentration employed of 100 μM. Moreover, we were able to follow in real-time the kinetics of internalization of our compounds by means of a live cell imaging technique. The intensity plot over different incubation times is displayed in Fig. S5b of the ESI.† We found out that the uptake of compound **3**, as an example, occurred within a short span of time upon incubation. A low intensity signal can be observed just a few seconds after the incubation while intense staining patterns can be clearly seen from the cytoplasmic region of the cells after 10 min of incubation and they increased over time for 1 hour (Fig. 5, complex **3**). We also observed a similar trend for compound **4** and **5** (see Fig. S6 and S7† respectively). By comparing the intensity

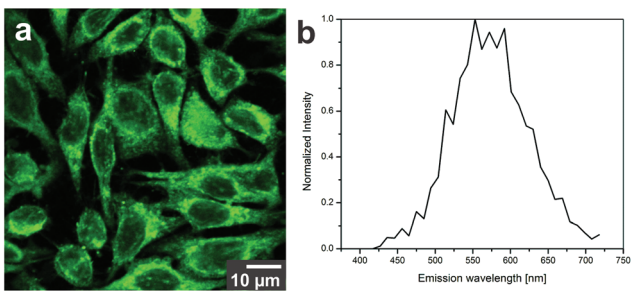

Fig. 3 (a) Fluorescence confocal image of HeLa cells after the incubation of compound **3** (50 μM in less than 1% DMSO containing PBS). (b) The emission spectrum recorded from the cytoplasm of the cells. The samples were excited at λ_{exc} = 405 nm.

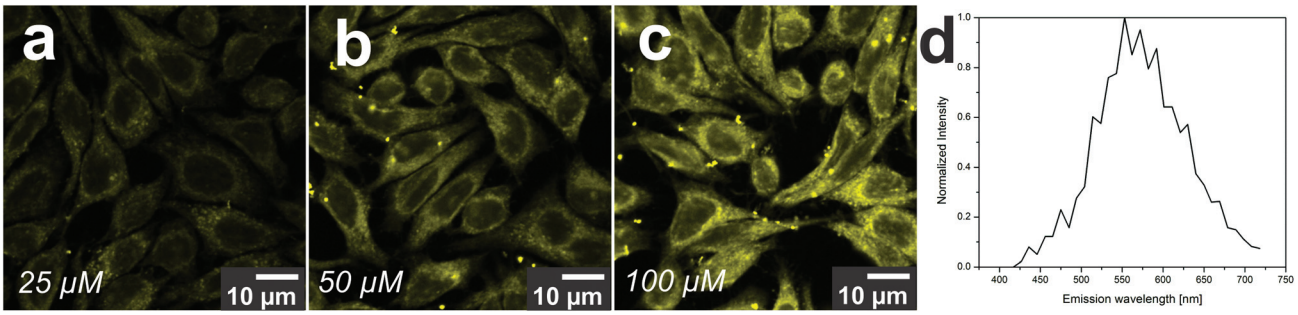

Fig. 4 Confocal images of HeLa cells after the incubation of compound **4** at different concentrations (a) 25, (b) 50, and (c) 100 μM in less than 1% v/v DMSO containing PBS. (d) The emission spectrum recorded from the cytoplasmic region of the cell. The samples were excited at λ_{exc} = 405 nm.

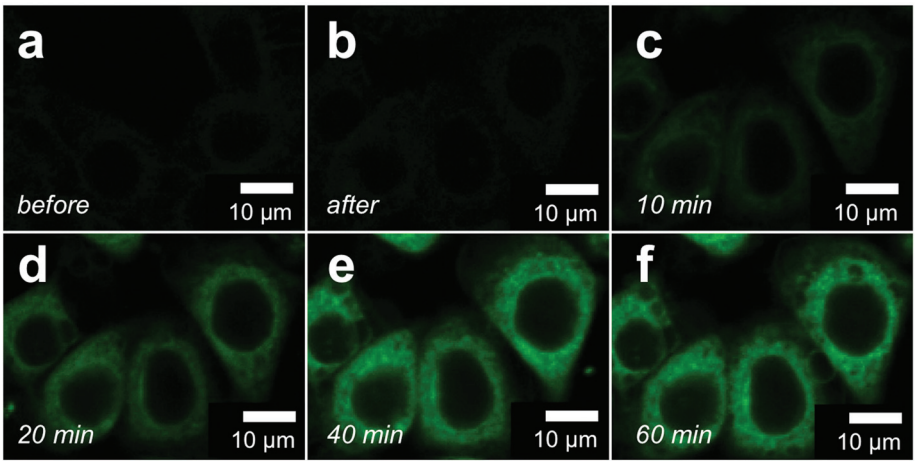

Fig. 5 Confocal images of HeLa cell line (a) before and (b–f) after addition of compound **3** at a concentration of 100 μM in less than 1% v/v DMSO containing PBS. Kinetics experiment shows fast internalization of the compound at different time periods (b) seconds, (c) 10 minutes, (d) 20 minutes, (e) 40 minutes, and (f) 1 hour after incubation. The samples were excited at λ_{exc} = 405 nm.

profile over time for all of the complexes, we found out that the emission signal for cells stained with complex **5** shows the steepest increase over time (Fig. S5b of the ESI†). Such a finding may underline a faster internalization process occurring for compound **5** compared to compound **3** and **4**, keeping in mind that the experimental conditions were maintained the same and the photophysical properties of the three complexes, especially in terms of the luminescence quantum yield, are comparable (see Fig. S5† and photophysical data listed in Table 1). The higher cellular uptake of the more hydrophilic complex **5** could be associated with an active transport mechanism. Nonetheless, the fast internalization time points towards the diffusion mechanism through the cell membrane. Further investigations in this direction are currently ongoing.

To further shed light on the ability of the presented complexes to act as bio-imaging probes in living cells, co-localization experiments were performed by means of co-staining experiments with DAPI for the nucleus, ER-Tracker™ Red for the endoplasmic reticulum and Phalloidin Alexa Fluor® 647 dye as the f-actin staining. As displayed in Fig. 6a–d, the results obtained with DAPI co-staining can exclude the presence of all complexes inside the nuclear region whereas a perfect overlapping with the signals derived from ER-Tracker™ Red (overlap coefficient 0.87) was observed, indicating its local-

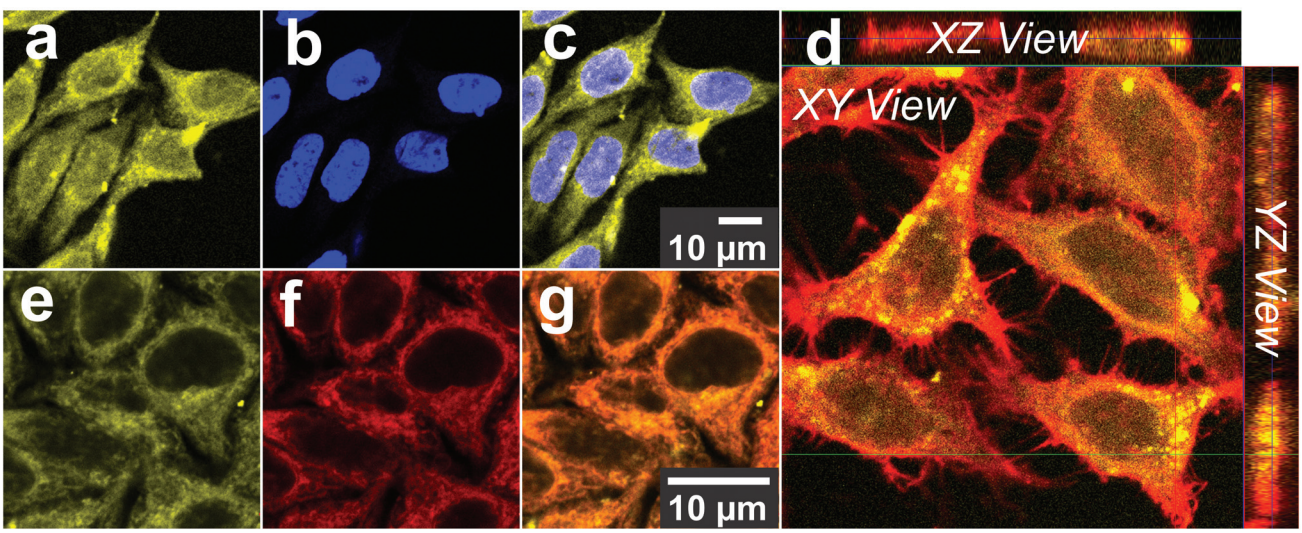

Fig. 6 Fluorescence confocal micrographs showing the distribution of compound **4** inside HeLa cells at a concentration of 100 μM in less than 1% DMSO containing PBS as the incubation media. (a) and (e) 4, (b) DAPI staining of nucleus, (c) overlay (a) and (b), (d) orthogonal view of the image showing 4 signals (yellow) coming from the inside of the cytoplasmic region of the cells which is stained with Phalloidin Alexa Fluor® 647 (red), (f) ER-Tracker™ Red stains the endoplasmic reticulum, (g) overlay (e) and (f). The excitation wavelength for DAPI and compound **4** was 405 nm, while ER-Tracker™ Red and Phalloidin Alexa Fluor® 647 were excited at 594 and 633 nm, respectively.

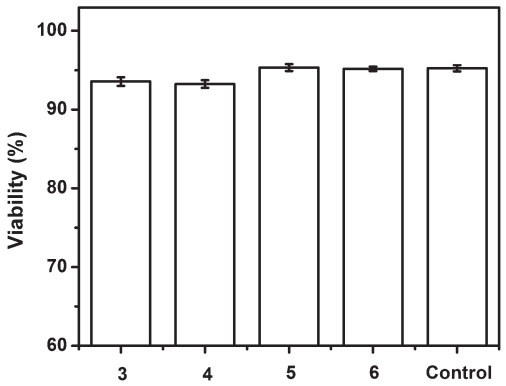

Fig. 7 Cellular viability studies after 1 hour incubation with different complexes at a concentration of 50 μM in <1% DMSO containing PBS. The compound name is indicated on the *x* axis.

ization in the endoplasmic reticulum (Fig. 6e–g).[18] Similar results were also obtained for compound **3** and **5**, as shown in Fig. S8 and S9 in the ESI.†

In sharp contrast, incubation with compound **6** of HeLa cells under identical conditions resulted in no emission being detected from the cells except for a typical autofluorescence signal derived from NADH and FAD molecules[19] (see Fig. S10, ESI†). Even though, it is still not clear if the compound was taken up but the emission was quenched in the cellular compartments due to quenching processes and aggregation phenomena or not taken up at all. However, its rather poor luminescence features make this compound much less attractive for bio-imaging purposes at this stage and it will not be further investigated.

Noteworthily, typical healthy cell shapes and no sign of apoptosis were observed during the incubation experiments. This observation demonstrates the very low degree of toxicity of the compounds inside the cellular compartments and organelles; a valuable feature for luminescent bio-imaging probes. To further quantify such a finding, the cellular viability assay based on electric current exclusion and pulse area analysis was performed by means of CASY® equipment and the results are depicted in Fig. 7. Interestingly, the number of viable cells after 1 hour incubation with complexes **3–6** is found to be close to the control experiments, confirming the low cytotoxicity of the complexes and their suitability as efficient phosphorescent labelling probes that can be used in cellular imaging applications.

Conclusions

Different glyco-conjugates based on luminescent dinuclear rhenium complexes have been synthesized using glucose or maltose derivatives and bio-orthogonal glyco-conjugation procedures. These new conjugates have been evaluated in terms of their optical properties and suitability as bio-imaging dyes in living HeLa cells. The conjugation with sugars increases the solubility of the complexes in aqueous media and does not appear to perturb the nature of the emitting excited state on the complex moiety. More importantly, it affords an amphiphilic character to the resulting glyco-conjugates, allowing the formation of soft aggregates, which display a higher photoluminescent quantum yield and a longer excited state lifetime than the corresponding parental luminescent rhenium carbonyl complex.

Cellular internalization experiments on human cervical adenocarcinoma cells (HeLa) have shown that these glyco-conjugates have fascinating bio-imaging properties, *i.e.* high cell permeability, organelle selectivity, low cytotoxicity, and fast internalization demonstrating their valuable suitability as efficient phosphorescent probes to be used in living cell imaging application.

Experimental

Supporting figures and synthetic procedures including NMR spectra can be found in the ESI.†

Materials and methods

Chemicals were purchased from commercial sources and used without further purification, unless otherwise indicated. When anhydrous conditions were required, the reactions were performed in oven-dried glassware under a nitrogen atmosphere. Anhydrous solvents were purchased from Sigma-Aldrich® with a content of water ≤0.005%. THF was dried over Na/benzophenone and freshly distilled prior to use. Thin-layer chromatography (TLC) was performed on Silica Gel 60 F254 plates or RP-C18 Silica plates (Merck) with UV detection (254 nm and 365 nm) or using appropriate developing solutions. Flash column chromatography was performed on silica gel 230–400 mesh (Merck), according to the procedure described in the literature. Automated flash chromatography was performed on a Biotage® Isolera™ Prime system. NMR experiments were recorded on a Bruker AVANCE 400 MHz instrument at 298 K. Chemical shifts (δ) are reported in ppm downfield from TMS as the internal standard, whereas coupling constants (J) are stated in Hz. The ^{1}H and ^{13}C-NMR resonances of compounds were assigned by means of COSY and HSQC experiments. Mass spectra were recorded on an Apex II ICR FTMS (ESI ionization-HRMS), Waters Micromass Q-TOF (ESI ionization-HRMS), ThermoFischer LCQ apparatus (ESI ionization) or Bruker Daltonics Microflex LT (MALDI-TOF apparatus). Specific optical rotation values were measured using a Perkin-Elmer 241, at 589 nm in a 1 mL cell. In the optimized copper(I)-catalyzed azide–alkyne cycloaddition (CuAAC) procedure, the starting materials and reagents were added to the reaction mixture as a solid or as a solution in water or THF. The water was degassed by bubbling with nitrogen and THF was freshly distilled. The reagents were added to the reaction vessel in the following order: multivalent scaffold (1 eq., solid or in THF), TBTA (0.2 eq., in THF), $CuSO_4 \cdot 5H_2O$ (0.1 eq., in H_2O), sodium ascorbate (0.4 eq., in H_2O) and finally the azide monovalent ligand (1.1 eq. per each triple bond, solid or in H_2O). The final

concentration of the multivalent scaffold was around 20 mM in a mixture of THF : H_2O (1 : 1) and the reaction was stirred overnight at room temperature under a nitrogen atmosphere, protected from light and monitored by mass spectrometry (MALDI-Tof) until completion. When RP-C18 chromatography was performed, the sample was loaded on a C18 prepacked sample and purified using a Biotage system (column SNAP KP-C18-HS, gradient elution H_2O : MeOH). Finally the solvent was removed by lyophilization obtaining the final purified product.

Synthesis

$[ReCl(CO)_5]$ and complex **1** were prepared according to a literature method.[12,20] Synthesis of 4-ethanoyl-5-ethyl-pyridazine was carried out according to a literature procedure,[15] involving the synthesis of 1,2,4,5-tetrazine (from hydrazine hydrate and formamidine acetate) as the first step followed by its reaction with the alkyne.

Complex 2. A sample of $[ReCl(CO)_5]$ (117.1 mg, 0.324 mmol) was dissolved in a toluene solution (20 mL) and treated with 0.5 eq. of 4-ethanoyl-5-ethyl-pyridazine (24.3 mg, 0.162 mmol). The solution was heated at the reflux temperature for three hours and then evaporated to dryness, giving a brownish solid. The desired product was isolated as a yellow solid from the crude by silica gel column chromatography using CH_2Cl_2 : AcOEt 4 : 1 as the eluent. IR (CH_2Cl_2) ν (CO): 2049 (m), 2033 (s), 1945 (s), 1914 (m) cm^{-1}. ^1H NMR (CD_2Cl_2, 300 K, 400 MHz) δH (ppm) 9.65 (s, 1H, H3-pydz), 9.49 (s, 1H, H6-pydz), 4.06 (m, 2H), 3.10 (t, 2H), 2.97 (q, 2H), 1.42 (t, 3H). Elemental Anal. Calcd for $C_{14}H_{12}Cl_2N_2O_7Re_2$: C 22.02, H 1.58, N 3.67. Found: C 22.12, H 1.53, N 3.65.

Compound 9. To a solution of penta-*O*-acetyl-D-glucose (**8**) (1 g, 2.67 mmol, 1 eq.) and 3-hexyn-1-ol (**7**) (365 μL, 3.2 mmol, 1.2 eq.) in anhydrous DCM (22 mL), BF_3–Et_2O (507 μL, 4.0 mmol, 1.5 eq.) was added at 0 °C under a nitrogen atmosphere. Then the mixture was slowly allowed to warm and stir for 4 h at room temperature until the reaction was complete (TLC hex : AcOEt 7 : 3 $R_{f\ prod.}$ = 0.26). Finally the reaction was quenched by addition of Et_3N (670 μL, 4.8 mmol, 1.8 eq.), stirred for additional 15 min and concentrated under reduced pressure. The crude was purified by flash chromatography (hexane : AcOEt gradient elution) affording a pure compound (**9**) (740 mg, 68%, β-anomer). ^1H NMR (400 MHz, $CDCl_3$) δ 5.20 (t, $J_{3,2}$ = 9.5 Hz, 1H, H_3), 5.08 (t, $J_{4,5}$ = 9.7 Hz, 1H, H4), 4.98 (dd, $J_{2,3}$ = 9.5 Hz, $J_{1,2}$ = 8.0 Hz, 1H, H2), 4.56 (d, $J_{1,2}$ = 8.0 Hz, 1H, H1), 4.26 (dd, $J_{6a,6b}$ = 12.3 Hz, $J_{6a,5}$ = 4.7 Hz, 1H, H6a), 4.13 (dd, $J_{6a,6b}$ = 12.3, $J_{6b,5}$ = 2.4 Hz, 1H, H6b), 3.89 (dt, $J_{7a,7b}$ = 9.8, $J_{7a,8}$ = 7.0 Hz, 1H, H7a), 3.69 (ddd, $J_{5,4}$ = 9.9 Hz, $J_{5,6a}$ = 4.7 Hz, $J_{5,6b}$ = 2.4 Hz, 1H, H5), 3.62 (dt, $J_{7a,7b}$ = 9.8, $J_{7b,8}$ = 7.5 Hz, 1H, H7b), 2.43 (tt, $J_{8,7}$ = 7.1 Hz, $J_{8,11}$ = 2.3 Hz, 2H, H8), 2.18–2.10 (m, 2H, H11), 2.09 (s, 3H, AcO), 2.05 (s, 3H, AcO), 2.02 (s, 3H, AcO), 2.00 (s, 3H, AcO), 1.10 (t, $J_{12,11}$ = 7.5 Hz, 3H, H12). 13C NMR (100 MHz, $CDCl_3$) δ 170.85, 170.46, 169.54, 169.50 (CO), 100.95 (C1), 83.21, 75.35 (C9, C10), 72.94 (C3), 71.97 (C5), 71.33 (C2), 68.81 (C7), 68.53 (C4), 62.07 (C6), 20.90, 20.81, 20.78, 20.76 (AcO), 20.24 (C8), 14.29 (C12), 12.52 (C11). MS (ESI) m/z calculated for $[C_{20}H_{28}O_{10}Na]^+$: 451.16, found: 451.4 $[M + Na]^+$. $[\alpha]_{25}^D$ = −17.85 (C = 0.685, CH_3Cl).

Compound 10. A solution of compound (**9**) (740 mg, 1.73 mmol) in freshly distilled MeOH (31.5 mL) was treated with a solution of NaOMe (3.5 mL, 1 M in MeOH). The reaction was stirred at room temperature under a nitrogen atmosphere monitoring the progress by TLC (hexane : AcOEt 1 : 1). After 1 h the reaction was complete. The mixture was diluted with MeOH and neutralized by addition of Amberlite IR 120-H^+ resin, then the beads were filtered off and washed with MeOH. Finally the solvent was removed under reduced pressure and the crude was purified by flash chromatography (DCM : MeOH 9 : 1) affording a pure compound (**10**) (420 mg, 93%). ^1H NMR (400 MHz, MeOD) δ 4.29 (d, $J_{1,2}$ = 7.8 Hz, 1H, H1), 3.98–3.81 (m, 2H, H6a, H7a), 3.72–3.56 (m, 2H, H6b, H7b), 3.37–3.32 (m, 1H, H3), 3.28–3.24 (m, 2H, H4, H5), 3.17 (dd, $J_{2,3}$ = 8.9, $J_{2,1}$ = 7.8 Hz, 1H, H2), 2.46 (tt, $J_{8,7}$ = 7.4, $J_{8,11}$ = 2.3 Hz, 2H, H8), 2.13 (qt, $J_{11,12}$ = 7.5, $J_{8,11}$ = 2.3 Hz, 2H, H11), 1.09 (t, $J_{11,12}$ = 7.5 Hz, 3H, H12). ^{13}C NMR (100 MHz, MeOD) δ 104.36 (C1), 83.52, 78.01 (C3), 77.98 (C4), 76.61, 75.01 (C2), 71.57 (C5), 69.59 (C7), 62.71 (C6), 20.86 (C8), 14.64 (C12), 13.03 (C11); MS (ESI) m/z calculated for $[C_{12}H_{20}O_6Na]^+$: 283.27, found: 283.3 $[M + Na]^+$. $[\alpha]_{25}^D$: −35.2 (C = 0.481, MeOH).

Compound 11. Synthesis of glycosylated pyridazine was carried out according to a literature procedure, involving the synthesis of 1,2,4,5-tetrazine (from hydrazine hydrate and formamidine acetate) as the first step followed by its reaction with the functionalized alkyne **10** (Scheme 1) The crude was purified by RP-18 chromatography (H_2O : MeOH gradient elution) affording a pure compound (**11**) (mg, 35% yield). ^1H NMR (400 MHz, MeOD) δ 9.07 (s, 1H, HAr), 8.96 (s, 1H, HAr), 4.31 (d, $J_{1,2}$ = 7.8 Hz, 1H, H1), 4.18 (dt, $J_{7a,7b}$ = 10.1, $J_{7a,8}$ = 6.5 Hz, 1H, H7a), 3.94–3.81 (m, 2H, H7b, H6a), 3.69–3.60 (m, 1H, H6b), 3.37–3.33 (m, 1H, H5), 3.26 (m, 2H, H3, H4), 3.15 (dd, $J_{2,3}$ = 9.1, $J_{1,2}$ = 7.8 Hz, 1H, H2), 3.08 (t, $J_{7,8}$ = 6.4 Hz, 2H, H8), 2.81 (q, $J_{11,12}$ = 7.6 Hz, 2H, H11), 1.29 (t, $J_{11,12}$ = 7.6, 3H, H12); ^{13}C NMR (100 MHz, MeOD) δ 153.58, 152.72 (CHAr), 144.85, 139.64 (CqAr), 104.42 (C1), 78.13, 78.05 (C4, C5), 75.00 (C2), 71.60 (C3), 69.01 (C7), 62.76 (C6), 30.56 (C8), 23.58 (C11), 14.22 (C12). MS (ESI) m/z calculated for $[C_{14}H_{22}N_2O_6Na]^+$: 337.32, found: 337.4 $[M + Na]^+$; $[\alpha]_{25}^D$: −16.01 (C = 0.316, MeOH).

Complex 3. Complex **3** (see Chart 3 for its structures and abbreviations) was prepared from $[ReCl(CO)_5]$, using the previously reported method. The crude was purified by RP-18 chromatography (H_2O : MeOH gradient elution) affording a pure compound (**3**) (mg, 12% yield). ^1H NMR (400 MHz, MeOD) δ 9.84 (s, 1H, HAr), 9.74 (s, 1H, HAr), 4.32 (d, $J_{1,2}$ = 7.6 Hz, 1H, H1), 4.24–4.14 (m, 1H, H7a), 4.08–3.99 (m, 1H, H7b), 3.86 (dd, $J_{6a,6b}$ = 11.7, $J_{6a,5}$ = 2.3 Hz, 1H, H6a), 3.56 (dd, $J_{6a,6b}$ = 11.7, $J_{6b,5}$ = 6.8 Hz, 1H, H6b), 3.36–3.15 (m, 8H, H2, H3, H4, H5, H8), 3.00 (q, $J_{11,12}$ = 7.6 Hz, 2H, H11), 1.37 (t, $J_{11,12}$ = 7.6 Hz, 3H, H12); ^{13}C NMR (100 MHz, MeOD) δ 195.79, 191.96 (CO), 164.48, 163.16 (CAr), 151.05, 146.43 (C9, C10), 105.11 (C1), 78.37, 78.14 (C4, C5), 74.68, 71.74 (C2, C3), 69.05 (C7), 63.03 (C6), 31.32 (C8), 24.07 (C11), 13.88 (C12); MS (ESI) 949.2 $[M + Na]^+$, HRMS (ESI) m/z calculated for $[C_{20}H_{22}Cl_2N_2O_{12}Re_2Na]^+$:

948.95311, found: 948.95418 $[M + Na]^+$ (error: 1.1 ppm); $[\alpha]_{25}^{D}$: + 6.21 (C = 0.43, MeOH).

Compound 13. To a solution of 2-(2-chloroethoxy)ethanol (**12**) (423 μL, 4 mmol, 1 eq.) in water (5 mL), NaN_3 (782 mg, 12 mmol, 3 eq.) and NaI (60 mg, 0.4 mmol, 0.1 eq.) were added. The reaction mixture was stirred at 60 °C for 96 h. The mixture was saturated with NaCl and extracted with DCM (3 × 10 mL), and the organic phase was dried over Na_2SO_4, filtered, concentrated under nitrogen flow and used without further purification.

Compound 14. To a solution of compound (**13**) (4 mmol, 1 eq.) in DCM (25 mL), TsCl (1.15 g, 6 mmol, 1.5 eq.) and then Et_3N (1.7 mL, 12 mmol, 3 eq.) were added under nitrogen at 0 °C, and then the mixture was stirred at r.t. for 3 h. The crude solution was washed with saturated $NaHCO_3$ (3 × 20 mL) and brine (20 mL), dried on anhydrous Na_2SO_4, filtered and evaporated under reduced pressure. Flash chromatography purification (hex : AcOEt gradient elution) gave a pure compound (**14**) (1.09 g, 80% yield). ^{1}H NMR (400 MHz, $CDCl_3$) δ 7.80 (d, J_{AB} = 8.2 Hz, 2H, AA′BB′, Ar–HAA′), 7.35 (d, J_{AB} = 8.2 Hz, 2H, AA′BB′, Ar–HBB′), 4.25–4.08 (m, 2H, H4), 3.76–3.64 (m, 2H, H3), 3.64–3.57 (m, 2H, H2), 3.32 (t, $J_{1,2}$ = 5.0 Hz, 2H, H1), 2.45 (s, 3H, Me); ^{13}C NMR (100 MHz, $CDCl_3$) δ 145.05, 133.03 (Cq), 129.99, 128.12 (CHAr), 70.31 (C2), 69.25 (C4), 68.83 (C3), 50.76 (C1), 21.78 (Me); MS (ESI) *m*/*z* calculated for $[C_{11}H_{15}N_3O_4SNa]^+$: 308.06, found: 308.1 $[M + Na]^+$.

***N*-Boc-*N*-methylhydroxylamine.** To solution of *N*-methylhydroxylamine hydrochloride (630 mg, 7.54 mmol, 1 eq.) in dry DCM (36 mL), di-*tert*-butyl dicarbonate (1.3 g, 6.03 mmol, 0.8 eq.) was added, and then the mixture was treated with Et_3N (1 mL, 7.54 mmol, 1 eq.) and stirred at r.t. under a nitrogen atmosphere for 4 hours. Finally, the crude solution was washed with 0.1 M $NaHSO_4$ (3 × 25 mL) and brine (3 × 25 mL). The organic phase was dried on anhydrous Na_2SO_4, filtered and evaporated under reduced pressure giving pure *N*-Boc-*N*-methylhydroxylamine (583 mg, 52% yield). ^{1}H NMR (400 MHz, $CDCl_3$) δ 6.68 (bs, 1H, OH), 3.15 (s, 3H, NMe), 1.49 (s, 9H, *t*Bu).

Compound 15. To a solution of *N*-Boc-*N*-methylhydroxylamine (360 mg, 2.45 mmol, 1.4 eq.) in dry THF (2 mL), DBU (393 μL, 2.63 mmol, 1.5 eq.) and a solution of compound **14** (500 mg, 1.75 mmol, 1 eq.) in dry THF (1.5 mL) were added. Then the mixture was stirred and left under the flow of nitrogen until the solvent was removed, and then the neat reaction was stirred overnight at room temperature. The crude was suspended in AcOEt (30 mL) and the organic phase was washed with 0.1 M $NaHSO_4$ (3 × 10 mL), 0.1 M NaOH (3 × 10 mL) and brine (10 mL), and then dried over anhydrous Na_2SO_4 and filtered. The evaporation of the solvent under reduced pressure gave a pure compound (**15**) (400 mg, 88% yield). ^{1}H NMR (400 MHz, $CDCl_3$) δ 4.05–3.97 (m, 2H, H4), 3.74–3.61 (m, 4H, H2, H3), 3.43–3.34 (m, 2H, H1), 3.10 (s, 3H, Me), 1.47 (s, 9H, *t*Bu). ^{13}C NMR (100 MHz, $CDCl_3$) δ 157.11 (CO), 81.44 (Cq), 73.68 (C1), 70.12, 68.92 (C2, C3), 50.83 (C1), 36.91 (NMe), 28.38 (*t*Bu). MS (ESI) *m*/*z* calculated for $[C_{10}H_{20}N_4O_4Na]^+$: 283.13, found: 283.1 $[M + Na]^+$.

Compound 16. To a solution of compound (**15**) (60 mg, 0.23 mmol, 1 eq.) in DCM (2 mL), PPh_3 (113 mg, 0.43 mmol, 1.9 eq.), Na_2CO_3 (46 mg, 0.23 mmol, 1 eq.) and H_2O (400 μL) were added, and then the reaction mixture was vigourously stirred at r.t. overnight. The solvents were removed under reduced pressure and the crude was purified by flash chromatography (eluent DCM : MeOH 9 : 1 + 1% 7 N NH_3 in MeOH) obtaining a pure compound (**16**) (46 mg, 85% yield) as a yellowish oil. ^{1}H NMR (400 MHz, MeOD) δ 4.02–3.97 (m, 2H, H4), 3.69–3.63 (m, 2H, H3), 3.53 (t, J = 5.3 Hz, 2H, H2), 3.11 (s, 3H, NMe), 2.79 (t, $J_{1,2}$ = 5.3 Hz, 2H, H1), 1.49 (s, 9H, *t*Bu). ^{13}C NMR (100 MHz, MeOD) δ 158.55 (CO), 82.73 (Cq), 74.63 (C4), 73.38 (C2), 69.57 (C3), 42.08 (C1), 37.04 (NMe), 28.52 (*t*Bu); MS (ESI) *m*/*z* calculated for $[C_{10}H_{23}N_2O_4]^+$: 235.30, found: 235.1 $[M + H]^+$.

Compound 17a. To a solution of compound (**1**) (48 mg, 62 μmol, 1.1 eq.) in dry DCM (2.5% DMA dry) (2 mL + 70 μL), HATU (32 mg, 85 μmol, 1.5 eq.) and then freshly distilled DIPEA (29 μL, 17 μmol, 3 eq.) were added under a nitrogen atmosphere. After 15 min a solution of compound (**16**) (13 mg, 56 μmol, 1 eq.) in dry DCM (600 μL) was added and the reaction was stirred at r.t. under nitrogen for 1 h. The crude was coevaporated with toluene and $CHCl_3$, and purified by flash chromatography (hexane : AcOEt gradient elution) obtaining a pure compound (**17a**) (47 mg, 72% yield). ^{1}H NMR (400 MHz, $CDCl_3$) δ 9.67–9.55 (m, 2H, H-10, H11), 8.00 (dd, $J_{9,10}$ = 5.9, $J_{9,11}$ = 2.3 Hz, 1H, H9), 7.10 (bt, 1H, NH), 4.01–3.94 (m, 2H, H1), 3.70–3.62 (m, 2H, H2), 3.62–3.56 (m, 2H, H3), 3.42 (m, 2H, H4), 3.13 (s, 3H, NMe), 2.98 (t, $J_{7,6}$ = 7.5 Hz, 2H, H7), 2.44–2.37 (m, 2H, H5), 2.20–2.10 (m, 2H, H6), 1.47 (s, 9H, O*t*Bu); ^{13}C NMR (100 MHz, $CDCl_3$) δ 193.62, 193.46, 190.66 (CORe), 171.63 (CONH), 163.02, 161.22 (C10, C11), 157.04 (OCON), 149.01 (C8), 132.00 (C9), 81.90 (Cq), 73.24 (C1), 69.54 (C3), 67.99 (C2), 39.12 (C4), 36.87 (NMe), 34.16 (C5), 31.94 (C7), 28.41 (*t*Bu), 25.13 (C6); MS (ESI) *m*/*z* calculated for $[C_{24}H_{30}Cl_2N_4O_{11}Re_2Na]^+$: 1017.02, found: 1017.2 $[M + Na]^+$ and 993.5 $[M - H]^-$.

Compound 17b. A solution of compound (**17a**) (47 mg, 47 μmol, 1 eq.) in dry DCM (2.4 mL) was treated with TFA (181 μL, 2.36 mmol, 50 eq.) under a nitrogen atmosphere at 0 °C, and then the mixture was stirred at room temperature for 1 hour until the reaction was complete (TLC, AcOEt : MeOH 9 : 1, $R_{f\ prod.}$ = 0.28). The crude was diluted with $CHCl_3$ and coevaporated with toluene (3×) and $CHCl_3$ (3×) affording compound **17b** in quantitative yield that was used without further purification. ^{1}H NMR (400 MHz, MeOD) δ 9.96 (dd, $J_{9,11}$ = 2.3 Hz, $J_{10,11}$ = 0.9 Hz, 1H, H11), 9.88 (dd, $J_{9,10}$ = 5.9 Hz, $J_{10,11}$ = 0.9 Hz, 1H, H10), 8.11 (dd, $J_{9,10}$ = 5.9 Hz, $J_{9,11}$ = 2.3 Hz, 1H, H9), 4.24–4.14 (m, 2H, H1), 3.80–3.71 (m, 2H, H2), 3.56 (t, $J_{3,4}$ = 5.5 Hz, 2H, H3), 3.37 (t, $J_{3,4}$ = 5.5 Hz, 2H, H4), 3.00–2.94 (m, 5H, NMe, H5), 2.35 (t, $J_{6,7}$ = 7.1 Hz, 2H, H7), 2.15–2.03 (m, 2H, H6). ^{13}C NMR (100 MHz, MeOD) δ 195.63, 191.77 (CO), 175.33 (CONH), 165.01 (C11), 163.12 (C10), 151.16 (C8), 133.64 (C9), 74.27 (C1), 71.38 (C3), 70.52 (C2), 40.25 (C4), 36.70 (NMe), 35.71 (C7), 32.73 (C5), 26.24 (C6).

Complex 4. To a solution of compound **17b** (23 mg, 22.8 μmol, 1 eq.) and D-glucose (12 mg, 69 μmol, 3 eq.) in dry

MeOH (230 μL), glacial AcOH (33 μL, 0.57 mmol, 25 eq.) was added and then the mixture was stirred at r.t. overnight. The crude mixture was directly loaded on a C-18 column and purified by RP-18 chromatography (H_2O : MeOH gradient elution) affording a pure compound (**4**) (15 mg, 62% yield). ^{1}H NMR (400 MHz, MeOD) δ 9.99 (dd, $J_{15,17}$ = 2.3 Hz, $J_{16,17}$ = 0.9 Hz, 1H, H17), 9.88 (dd, $J_{15,16}$ = 5.9 Hz, $J_{16,17}$ = 0.9 Hz, 1H, H16), 8.14 (dd, $J_{15,16}$ = 5.9 Hz, $J_{15,17}$ = 2.3 Hz, 1H, H15), 8.02 (bt, $J_{NH,10}$ = 5.7 Hz, 1H, NH), 3.99 (d, $J_{1,2}$ = 8.9 Hz, 1H, H1), 3.92 (t, $J_{7,8}$ = 4.5 Hz, 2H, H7), 3.86 (dd, $J_{6a,6b}$ = 12.0 Hz, $J_{5,6a}$ = 2.2 Hz, 1H, H6a), 3.70 (dd, $J_{6a,6b}$ = 12.0, $J_{5,6b}$ = 5.1 Hz, 1H, H6b), 3.67–3.60 (m, 2H, H8), 3.55 (t, $J_{9,10}$ = 5.2 Hz, 2H, H9), 3.49 (t, $J_{1,2}$ = 8.9 Hz, 1H, H2), 3.42–3.32 (m, 4H, H3, H4, H10), 3.23 (ddd, $J_{4,5}$ = 9.5 Hz, $J_{5,6b}$ = 5.1 Hz, $J_{5,6a}$ = 2.2 Hz, 1H, H5), 3.02–2.94 (m, 2H, H11), 2.74 (s, 3H, NMe), 2.42–2.32 (m, 2H, H13), 2.15–2.02 (m, 2H, H12). ^{13}C NMR (100 MHz, MeOD) δ 195.68, 191.78 (CO), 174.98 (CONH), 165.04, 163.15 (C16, C17), 151.28 (Cq), 133.69 (C15), 95.45 (C1), 79.61 (C4), 79.25 (C5), 73.04 (C7), 71.61 (C2), 71.27 (C3), 70.39 (C9), 70.16 (C8), 62.79 (C6), 40.44 (C10), 39.23 (NMe), 35.75 (C13), 32.69 (C11), 26.35 (C12). HRMS (ESI) *m*/*z* calculated for $[C_{25}H_{32}Cl_2N_4O_{14}Re_2Na]^+$: 1079.02751, found: 1079.02718 $[M + Na]^+$ (error: −0.3 ppm); $[\alpha]_{25}^D$: −3.03 (C = 0.515, MeOH).

Complex 5. To a solution of compound **17b** (23 mg, 22.8 μmol, 1 eq.) and D-maltose (25 mg, 69 μmol, 3 eq.) in dry MeOH (230 μL), glacial AcOH (33 μL, 0.57 mmol, 25 eq.) was added and then the mixture was stirred overnight at room temperature. The crude mixture was directly loaded on a C-18 column and purified by RP-18 chromatography (H_2O : MeOH gradient elution) affording a pure compound (**5**) (15 mg, 62% yield). ^{1}H NMR (400 MHz, MeOD) δ 9.99 (dd, $J_{15,17}$ = 2.3 Hz, $J_{16,17}$ = 0.9 Hz, 1H, H17), 9.88 (dd, $J_{15,16}$ = 5.9 Hz, $J_{16,17}$ = 0.9 Hz, 1H, H16), 8.15 (dd, $J_{15,16}$ = 5.9, $J_{15,17}$ = 2.3 Hz, 1H, H15), 8.04 (bt, $J_{NH,10}$ = 5.4 Hz, 1H, NH), 5.16 (d, $J_{1',2'}$ = 3.8 Hz, 1H, H1′), 4.01 (d, $J_{1,2}$ = 8.9 Hz, 1H, H1), 3.92 (t, $J_{7,8}$ = 4.4 Hz, 2H, H7), 3.89–3.79 (m, 2H, H6a, H6′ab), 3.72–3.52 (m, 10H, H8, H6b, H2, H3, H3′, H4, H4′, H9), 3.45 (dd, $J_{2',3'}$ = 9.7, $J_{1',2'}$ 3.8 Hz, 1H, H2′), 3.41–3.33 (m, 3H, H10, H5), 3.29–3.23 (m, 2H, H5′), 3.01–2.94 (m, 2H, H11), 2.75 (s, 3H, NMe), 2.38 (t, $J_{12,13}$ = 7.1 Hz, 2H, H13), 2.14–2.04 (m, 2H, H12). ^{13}C NMR (100 MHz, MeOD) δ 195.67, 195.60, 191.78, 191.71 (CO), 174.98 (CONH), 165.03, 163.17 (C16, C17), 151.27 (C14), 133.75 (C15), 102.93 (C1), 95.38 (C1′), 81.06, 78.96, 78.21, 75.09, 74.80, 74.19, 73.06 (C7), 71.47, 71.19, 70.41 (C8), 70.16 (C9), 62.72 (C6), 62.28 (C6′), 40.43 (C10), 39.38 (NMe), 35.77 (C13), 32.70 (C11), 26.38 (C12). HRMS (ESI) *m*/*z* calculated for $[C_{31}H_{48}Cl_2N_4O_{19}Re_2Na]^+$: 1241.08057, found 1241.08278 $[M + Na]^+$ (error: 1.8 ppm). $[\alpha]_{25}^D$: +15.54 (C = 0.605, MeOH).

Compound 6. To a solution of compound **1** (18 mg, 23 μmol, 1.2 eq.) and HATU (11 mg, 29 μmol, 1.5 eq.) in DMA dry (600 μL), freshly distilled DIPEA (10 μL, 57 μmol, 3 eq.) was added under a nitrogen atmosphere. After 15 min a solution of compound (**21**) (24 mg, 19 μmol, 1 eq.) in dry DMA (400 μL) was added and the reaction was stirred at r.t. under nitrogen for 1 h. The crude was directly loaded on a C-18 column and purified by RP-18 chromatography (H_2O : MeOH gradient elution) obtaining a pure compound (**6**) (26 mg, 68% yield). ^{1}H NMR (400 MHz, MeOD) δ 10.00 (dd, J = 2.2, 0.9 Hz, 1H, H27), 9.89 (dd, J = 5.9, 0.9 Hz, 1H, H26), 8.14 (dd, J = 5.9, 2.3 Hz, 1H, H25), 8.03 (s, J = 6.9 Hz, 3H, H11), 4.60–4.55 (m, 6H, H10), 4.53 (s, 6H, H13), 4.29 (d, J = 7.8 Hz, 3H, H1), 4.01–3.94 (m, 3H, H7a), 3.93–3.89 (m, 6H, H9), 3.89–3.85 (m, 3H, H6a), 3.74–3.63 (m, 14H, H6b, H7b, H8, H19), 3.56–3.48 (m, 4H, H17, H18), 3.46 (s, 6H, H14), 3.42 (s, 2H, H16), 3.39–3.36 (m, 3H, H3), 3.35–3.32 (m, 2H, H20), 3.30–3.25 (m, 6H, H4, H5), 3.20 (dd, J = 9.1, 7.8 Hz, 3H, H2), 3.02–2.91 (m, 2H, H21), 2.35 (t, J = 7.1 Hz, 2H, H23), 2.12–2.02 (m, 2H, H22); 13C NMR (100 MHz, MeOD) δ 195.69, 195.61, 191.79, 191.71 (ReCO), 174.92 (CONH), 165.09, 163.20 (C26, C27), 151.28 (C24), 146.02 (C12), 133.75 (C25), 125.99 (C11), 104.48 (C1), 78.05, 78.01 (C3, C5), 75.11 (C2), 72.18 (C17), 71.64 (C4), 71.38 (C8), 71.25 (C18), 70.81 (C16), 70.51 (C19), 70.34 (C9), 70.03 (C14), 69.81 (C7), 65.32 (C13), 62.77 (C6), 51.35 (C10), 46.58 (C15), 40.49 (C20), 35.75 (C22), 32.69 (C21), 26.31 (C22); HRMS (ESI-Qtof) *m*/*z* calculated for $[C_{62}H_{92}Cl_{12}N_{12}O_{33}Re_2Na_2]^{2+}$: 1011.2061, found: 1011.1946 $[M + 2Na]^{2+}$ (error: 11 ppm); $[\alpha]_{25}^D$: −12.43 (C = 0.725, MeOH).

Photophysical characterization

Steady-state measurements. Absorption spectra were measured on a double-beam Shimadzu UV-3600 UV-vis-NIR spectrophotometer and baseline corrected. Steady-state emission spectra were recorded on a HORIBA Jobin-Yvon IBH FL-322 Fluorolog 3 spectrometer equipped with a 450 W xenon arc lamp and a TBX-4-X single-photon-counting as an excitation source and a detector, respectively. Emission spectra were corrected for source intensity (lamp and grating) and emission spectral response (detector and grating) by standard correction curves. The quantum yield measurements were performed by using a Hamamatsu Photonics absolute photoluminescence quantum yield system Quantaurus C11347-11 equipped with a continuous wave xenon light source (150 W), a motorized monochromator, a CCD photonic multichannel analyzer and employing a commercially available dedicated measurement software (Hamamatsu Photonics, Japan). The photoluminescence quantum yields were measured exciting the samples between 380–420 nm.

Lifetime measurements. Time-resolved measurements were performed using either time-correlated single-photon counting (TCSPC) electronics PicoHarp300 or Multi Channel Scaling (MCS) electronics NanoHarp 250 of PicoQuant FluoTime 300 (PicoQuant GmbH, Germany), equipped with a PDL 820 laser pulse driver. A pulsed laser diode LDH-P-C-405 (λ_{ex} = 405 nm, pulse FWHM <70 ps, repetition rate 200 kHz–40 MHz) was used to excite the sample and was mounted directly on the sample chamber at 90°. The photons were collected by using a PMA-C-192 photomultiplier (PMT) single-photon-counting detector. The data were acquired by using the commercially available software EasyTau (PicoQuant GmbH, Germany), while data analysis was performed using the commercially available software FluoFit (PicoQuant GmbH, Germany). The quality of the fit was assessed by minimizing the reduced χ^2 function (χ^2 < 1.2 and <1.5 for mono- and bi-exponential

model, respectively) and by visual inspection of the random distribution of the weighed residuals. For multi-exponential decays, the intensity, namely $I(t)$, has been assumed to decay as the sum of individual single exponential decays (eqn (1)):

$$I(t) = \sum_{i=1}^{n} \alpha_i \exp\left(-\frac{t}{\tau_i}\right) \quad (1)$$

where τ_i are the decay times and α_i are the amplitude of the components at $t = 0$. In the tables, the percentages of the pre-exponential factors, α_i, are listed upon normalization.

Fluorescence confocal microscopy

The experiments were carried out by incubating approximately 50 000 HeLa cells with various concentrations of compound solutions (25–100 μM in less than 1% v/v of DMSO/Phosphate Buffer Saline, PBS) for 1 h under normal biological conditions (37 °C and 5% CO_2). After the incubation, the stained cells were imaged directly using a fluorescence confocal microscopy setup. All of the fluorescence images were obtained by using a Zeiss LSM 710 confocal microscope set up with a 63× magnification, and a numerical aperture, NA, 1.3 of Zeiss LCI Plan-NEOFLUAR water immersion objective lens (Zeiss GmbH) equipped with a spectrometer. Image acquisition was directly performed by exciting the samples using a continuous wave (cw) laser at 405 nm. The emission of the complexes was collected in the range from 540 to 720 nm and also scanned in lambda-mode (for acquiring the emission spectra). For co-localization experiments, the samples previously co-stained with different dyes, DAPI (excitation/emission wavelength: 358 nm/461 nm), ER Tracker Red (excitation/emission wavelength: 587 nm/615 nm), and Alexa Fluor® 647 Phalloidin (excitation/emission wavelength: 650 nm/668 nm) were excited independently at 405, 594 and 633 nm, and the emission signals were collected according to their corresponding emission profiles. Image processing was performed by using Zen 2011 software (Zeiss GmbH). False colour images were adjusted to better distinguish different complexes and complexes from cellular organelles.

Cell culture

All materials for cell culture were purchased from Gibco. Human cervical carcinoma, HeLa, cells were cultured in media containing 88% Dulbecco's Modified Eagle Medium (DMEM), 10% Fetal Bovine Serum (FBS), 1% penicillin–streptomycin and 1% L-glutamine (200 mM) at 37 °C and under 5% CO_2 conditions for 48 hours until reaching 70 to 80% cell confluency. Subsequently, the cells were washed twice with Phosphate Buffer Solution (PBS, Gibco), trypsinated and approximately 50 000 cells were reseeded on a monolayer glass cover slip in a six-well plate culture dish and glass bottom dishes (MatTek). Fresh culture media (2 mL) was added gently and the cells were grown overnight.

Rhenium complex incubation

The culture media was removed and 2 mL of a new staining solution containing the corresponding rhenium complexes (50 μM in less than 1% DMSO containing PBS) were gently added onto cells. After incubation at 37 °C for 1 hour, the incubating media was removed and the cell layer on glass cover slips was gently washed (three times) with PBS and fixed with 4% paraformaldehyde (PFA) in PBS solution for 10 min.

Kinetic of internalization

The culture media of live cells grown onto glass bottom dishes was removed and 2 mL of the complex staining solution (100 μM in less than 1% DMSO containing PBS) was added. The cells were subsequently imaged by using a fluorescence confocal microscopy setup for a ten-minute acquisition time for a total duration of 60 minutes.

Organelle staining

The cell layer was washed twice with PBS and kept in 0.1% Triton X-100 (Sigma Aldrich) in PBS for 5 minutes and afterwards in 1% bovine serum albumin, BSA (Sigma Aldrich), in PBS for 20 min. The cell layer on the glass cover slip was stained with Phalloidin Alexa Fluor® 647 (Invitrogen), for f-actin/membrane staining, for 20 min, in the dark at room temperature, and washed two times with PBS. For visualizing the nuclear region, the cell nucleus was stained with 4′,6-diamidino-2-phenylindole carboxamidine (DAPI) and washed twice with PBS. In the case of **4**, ER Tracker Red dye (Invitrogen) was added to visualize the endoplasmic reticulum. The cover slips were mounted onto glass slides for microscopy measurements.

Cell viability studies

Cellular viability was measured by using an automatic cell counter CASY (Roche Innovatis AG, Bielefeld, Germany). Approximately 50 000 cells were grown in 2 ml of culture media in 6 well plates at 37 °C, in a 5% CO_2 environment for 48 hours. The culture media was removed and replaced with 1 ml staining solution of complex **2**, **3**, **4**, and **5** (50 μM in less than 1% DMSO in PBS). Subsequently after 1 hour of incubation, the staining solution was transferred to Eppendorf tubes and 0.5 ml of trypsin were added. To detach the cell from the surface of the plate, the cells were incubated for 5 minutes under the same conditions mentioned before. Subsequently, 0.5 ml of PBS was added to neutralize trypsin. The cell suspensions together with the first solutions were collected and removed into an Eppendorf tube. 100 μl of the cell suspension was dissolved in 10 ml of CASY ton solution and measurement was performed. The positive control of the cells grown without the complexes was also performed. All experiments were repeated 3 times.

Author contribution

A. P., A. A., and D. S. contributed equally to the work as follows: A. P. planned and performed the synthesis of all the compounds and of the complexes, supervised by A. B.; A. A. provided the spectroscopic and photophysical characteriz-

ation of the conjugates, supervised by M. M.; D. S. performed cellular uptake experiments and acquired the confocal microscopy images, all supervised by L. D. C. M. P., M. M., A. P., D. S. and A. B. planned the experiments, analysed and discussed the data and wrote the paper.

Acknowledgements

The University of Strasbourg is kindly acknowledged for financial support.

Notes and references

1 (*a*) B. Imperiali, *J. Am. Chem. Soc.*, 2012, **134**, 17835–17839; (*b*) W. H. Kim, J. Lee, D.-W. Jung and D. R. Williams, *Sensors*, 2012, **12**, 5005–5027.

2 (*a*) G. Jaouen, *Bioorganometallics II*, Wiley-VCH, Weinheim, Germany, 2015; (*b*) F. L. Thorp-Greenwood, M. P. Coogan, L. Mishra, N. Kumari, G. Rai and S. Saripella, *New J. Chem.*, 2012, **36**, 64–72; (*c*) Q. Zhao, C. Huang and F. Li, *Chem. Soc. Rev.*, 2011, **40**, 2508–2524; (*d*) F. L. Thorp-Greenwood, R. G. Balasingham and M. P. Coogan, *J. Organomet. Chem.*, 2012, **714**, 12–21.

3 (*a*) V. Fernández-Moreira, F. L. Thorp-Greenwood and M. P. Coogan, *Chem. Commun.*, 2010, **46**, 186–202; (*b*) E. Baggaleya, J. A. Weinstein and J. A. G. William, *Coord. Chem. Rev.*, 2012, **256**, 1762–1785; (*c*) M. Mauro, A. Aliprandi, D. Septiadi, N. S. Kehr and L. De Cola, *Chem. Soc. Rev.*, 2014, **43**, 4144–4166 and ref therein; (*d*) D. Sepiadi, A. Aliprandi, M. Mauro and L. De Cola, *RSC Adv.*, 2014, **4**, 25709–25718.

4 J.-J. Chen, J. Jing, H. Chang, Y. Rong, Y. Hai, J. Tang, J.-L. Zhang and P. Xu, *Autophagy*, 2013, **9**, 894–904.

5 (*a*) M. Gottschaldt, U. S. Schubert, S. Rau, S. Yano, J. G. Vos, T. Kroll, J. Clement and I. Hilger, *ChemBioChem*, 2010, **11**, 649–652; (*b*) D. Grunstein, M. Maglinao, R. Kikkeri, M. Collot, K. Barylyuk, B. Lepenies, F. Kamena, R. Zenobi and P. H. Seeberger, *J. Am. Chem. Soc.*, 2011, **133**, 13957–13966; (*c*) R. Kikkeri, X. Liu, A. Adibekian, Y.-H. Tsai and P. H. Seeberger, *Chem. Commun.*, 2010, **46**, 2197–2199; (*d*) T. Okada, T. Makino and N. Minoura, *Bioconjugate Chem.*, 2009, **20**, 1296–1298.

6 (*a*) L. Hua-Wei, K. Y. Zhang, W. H.-T. Law and K. K.-W. Lo, *Organometallics*, 2010, **29**, 3474–3476; (*b*) M.-J. Li, P. Jiao, W. He, C. Yi, C.-W. Li, X. Chen, G.-N. Chen and M. Yang, *Eur. J. Inorg. Chem.*, 2011, **2**, 197–200; (*c*) W. H.-T. Law, L. C.-C. Lee, M.-W. Louie, H.-W. Liu, T. W.-H. Ang and K. K.-W. Lo, *Inorg. Chem.*, 2013, **52**, 13029–13041.

7 D.-L. Ma, T. Y.-T. Shum, F. Zhang, C.-M. Che and M. Yang, *Chem. Commun.*, 2005, 4675–4677.

8 (*a*) S. R. Banerjee, J. W. Babich and J. Zubieta, *Inorg. Chim. Acta*, 2006, **359**, 1603–1612; (*b*) S. R. Bayly, C. L. Fisher, T. Storr, M. J. Adam and C. Orvig, *Bioconjugate Chem.*, 2004, **15**, 923–926; (*c*) T. Storr, M. Obata, C. L. Fisher, S. R. Bayly, D. E. Green, I. BrudziÇska, Y. Mikata, B. O. Patrick, M. J. Adam, S. Yano and C. Orvig, *Chem. Eur. J.*, 2005, **11**, 195–203; (*d*) J. Petrig, R. Schibli, C. Dumas, R. Alberto and P. A. Schubiger, *Chem. – Eur. J.*, 2001, **7**, 1868–1973; (*e*) T. Storr, C. L. Fisher, Y. Mikata, S. Yano, M. J. Adam and C. Orvig, *Dalton Trans.*, 2005, 654–655; (*f*) T. Storr, Y. Sugai, C. A. Barta, Y. Mikata, M. J. Adam, S. Yano and C. Orvig, *Inorg. Chem.*, 2005, **44**, 2698–2705; (*g*) C. L. Ferreira, C. B. Ewart, S. R. Bayly, B. O. Patrick, J. Steele, M. J. Adam and C. Orvig, *Inorg. Chem.*, 2006, **45**, 6979–6987; (*h*) T. L. Mindt, H. Struthers, L. Brans, T. Anguelov, C. Schweinsberg, V. Maes, D. Tourwé and R. Schibli, *J. Am. Chem. Soc.*, 2006, **128**, 15096–15097.

9 (*a*) Y. Mikata, K. Takahashi, Y. Noguchi, M. Naemura, A. Ugai, S. Itami, K. Yasuda, S. Tamotsu, T. Matsuo and T. Storr, *Eur. J. Inorg. Chem.*, 2012, **2**, 217–225; (*b*) M.-W. Louie, H.-W. Liu, M. Ho.-C. Lam, Y.-W. Lam and K. K.-W. Lo, *Chem. – Eur. J.*, 2011, **17**, 8304–8308; (*c*) K. Y. Zhang, K. K.-S. Tso, M.-W. Louie, H.-W. Liu and K. K.-W. Lo, *Organometallics*, 2013, **32**, 5098–5102.

10 (*a*) D. Donghi, G. D'Alfonso, M. Mauro, M. Panigati, P. Mercandelli, A. Sironi, P. Mussini and L. D'Alfonso, *Inorg. Chem.*, 2008, **28**, 4243–4255; (*b*) M. Panigati, M. Mauro, D. Donghi, P. Mercandelli, P. Mussini, L. De Cola and G. D'Alfonso, *Coord. Chem. Rev.*, 2012, **256**, 1621–1643.

11 (*a*) M. Mauro, E. Quartapelle Procopio, Y. Sun, C. H. Chien, D. Donghi, M. Panigati, P. Mercandelli, P. Mussini, G. D'Alfonso and L. De Cola, *Adv. Funct. Mater.*, 2009, **19**, 2607–2614; (*b*) M. Mauro, C.-H. Yang, C.-Y. Shin, M. Panigati, C.-H. Chang, G. D'Alfonso and L. De Cola, *Adv. Mater.*, 2012, **24**, 2054–2058.

12 (*a*) E. Ferri, D. Donghi, M. Panigati, G. Prencipe, L. D'Alfonso, I. Zanoni, C. Baldoli, S. Maiorana, G. D'Alfonso and E. Licandro, *Chem. Commun.*, 2010, **46**, 6255–6257; (*b*) C. Mari, M. Panigati, L. D'Alfonso, I. Zanoni, D. Donghi, L. Sironi, M. Collini, S. Maiorana, C. Baldoli, G. D'Alfonso and E. Licandro, *Organometallics*, 2012, **31**, 5918–5928.

13 A. J. Amoroso, M. P. Coogan, J. E. Dunne, V. Fernandez-Moreira, J. B. Hess, A. J. Hayes, D. Lloyd, C. Millet, S. J. A. Pope and C. Williams, *Chem. Commun.*, 2007, **29**, 3066–3068.

14 (*a*) B. R. Griffith, J. M. Langenhan and J. S. Thorson, *Curr. Opin. Biotechnol.*, 2005, **16**, 622–630; (*b*) J. M. Langenhan, B. R. Griffith and J. S. Thorson, *J. Nat. Prod.*, 2005, **68**, 1696–1711.

15 J. Sauer, D. K. Heldmann, J. Hetzenegger, J. Krauthan, H. Sichert and J. Schuster, *Eur. J. Org. Chem.*, 1998, 2885–2896.

16 (*a*) F. Peri, P. Dumy and M. Mutter, *Tetrahedron*, 1998, **54**, 12269–12278; (*b*) A. Palmioli, E. Sacco, S. Abraham, C. J. Thomas, A. D. Domizio, L. D. Gioia, V. Gaponenko, M. Vanoni and F. Peri, *Bioorg. Med. Chem. Lett.*, 2009, **19**, 4217–4222; (*c*) E. Sacco, S. J. Abraham, A. Palmioli, G. Damore, A. Bargna, E. Mazzoleni, V. Gaponenko, M. Vanoni and F. Peri, *MedChemComm*, 2011, **2**, 396–401.

17 C. Cebrián, M. Natali, D. Villa, M. Panigati, M. Mauro, G. D'Alfonso and L. De Cola, *Nanoscale*, 2015, **7**, 12000–12009.
18 M. Csala, P. Marcolongo, B. Lizák, S. Senesi, E. Margittai, R. Fulceri, J. É. Magyar, A. Benedetti and G. Bánhegyi, *Biochim. Biophys. Acta*, 2007, **1768**, 1325–1341.
19 (*a*) H. Andersson, T. Baechi, M. Hoechl and C. Richter, *J. Microsc.*, 1998, **191**, 1–7; (*b*) J. E. Aubin, *J. Histochem. Cytochem.*, 1979, **27**, 36–43.
20 S. P. Schmidt, W. C. Trogler and F. Basolo, *Inorg. Synth.*, 1985, **23**, 41.